Comparative Medicine
Copyright 2004
by the American Association for Laboratory Animal Science

Vol 54, No 6
December 2004
Pages 681-689

Pathogenesis of Enterotropic Mouse Hepatitis Virus in Immunocompetent and Immunodeficient Mice

Susan R. Compton, PhD,* Lisa J. Ball-Goodrich, PhD, Linda K. Johnson, DVM, Elizabeth A. Johnson, Frank X. Paturzo, and James D. Macy, DVM

Mouse hepatitis virus (MHV) is one of the most prevalent viruses infecting laboratory mice. Most natural infections are caused by enterotropic strains. Experiments were done to compare the pathogenesis of enterotropic strain MHV-Y in immunocompetent BALB/c and C57BL/6 mice with that in B and T cell-deficient mice. In situ hybridization was used to identify sites of virus replication, and reverse transcriptase-polymerase chain reaction analysis was used to detect viral RNA in feces and blood. MHV-Y caused acute subclinical infections restricted to the gastrointestinal tract in BALB/c and C57BL/6 mice. Viral RNA was detected in small intestine and associated lymphoid tissues of immunocompetent mice for 1 week and in cecum and colon for 2 weeks. Infected B cell-deficient mice developed chronic subclinical infection also restricted to the gastrointestinal tract. Viral RNA was detected in the small intestine, cecum, colon, and feces for 7 to 8 weeks. In contrast, infected T cell-deficient mice developed multisystemic lethal infection. During the first week, viral RNA was restricted to the gastrointestinal tract. However, by 2 weeks, mice developed peritonitis, and viral RNA was detected in mesentery and visceral peritoneum. Three to four weeks after virus inoculation, T cell-deficient mice became moribund and viral RNA was detected in multiple organ systems. These results suggest that B cells promote clearance of MHV-Y from intestinal mucosa and that T cells are required to prevent dissemination of MHV-Y from the gastrointestinal tract and associated lymphoid tissues.

Mouse hepatitis virus (MHV), the singular name for a diverse group of murine coronaviruses, causes a spectrum of disease that ranges from subclinical infection to enteritis, hepatitis, and encephalitis. Strains of MHV are classified into enterotropic or polytropic biotypes on the basis of their predominant sites of replication (17). Enterotropic strains such as MHV-Y cause acute subclinical infection in adult immunocompetent mice and rarely disseminate to other organs (3). In contrast, polytropic MHV strains cause acute or chronic infection in adult immunocompetent mice, with dissemination to multiple organs. In contemporary mouse colonies, natural infections with enterotropic MHV strains greatly outnumber those with polytropic MHV strains (17). Infection with MHV is still one of the most prevalent viral infections of laboratory mice (18). It is a major concern in laboratory animal colonies because it can disrupt mouse-based research through clinical disease or alteration of immunologic responses.

The principal site of replication for enterotropic MHV-Y is enterocytes of the distal portion of the small intestine and the cecum and ascending colon (3). Infection of juvenile and adult immunocompetent mice results in localized intestinal infection with subclinical disease. However, infection of neonatal mice results in severe enteritis and mortality (3), whereas infection of immunodeficient mice can result in multisystemic, chronic infection, with persistent viral shedding and mortality (4, 11).

Previous pathogenesis studies of enterotropic MHV were performed when many academic and commercial mouse colonies were endemically infected with *Helicobacter hepaticus* or other *Helicobacter* species (37). We confirmed, by use of polymerase chain reaction (PCR) analysis, that initial MHV-Y intestinal stocks used for experimentally induced infections were positive for *H. hepaticus* DNA (3, 10), suggesting that relevant MHV-Y studies may have been confounded by co-infection with *Helicobacter* sp. Recently, we reported that the pathogenesis of enterotropic MHV-G in mice deficient in interferon-γ was altered by *H. hepaticus* co-infection (11), supporting concerns about the potential impact of *Helicobacter* infection on the pathogenesis of MHV-Y in previously published studies of BALB/c mice. To our knowledge, the pathogenesis of enterotropic MHV has not been examined in C57BL/6 mice, the most common parental strain of genetically engineered mice. Therefore, we performed pathogenesis studies in *Helicobacter*-free BALB/c and C57BL/6 mice to confirm the sites of MHV-Y infection.

Although enterotropic MHV outbreaks indicate that infection (4) of athymic mice causes disseminated and lethal infection and subclinical persistent infection in mice with a rearranged T-cell receptor β-chain, the pathogenesis of enterotropic MHV strains in immunologically dysfunctional mice is not clear (35). To better understand the impact of specific immunologic deficiencies on enterotropic MHV infection, we performed a pathogenesis study of MHV-Y infection in B and T cell-deficient mice.

Materials and Methods

Mice. Four- to six-week-old female inbred BALB/cJ, C57BL/6J, B6.129S2-Igh-6^{tm1Cgn} (μMT), and B6.129P2-Tcrb^{tm1Mom} Tcrd^{tm1Mom} (Tcrβδ^{-}) mice were obtained from The Jackson Laboratories (Bar Harbor, Maine). Mice were seronegative for MHV, ectromelia virus, lymphocytic choriomeningitis virus, mouse minute virus, mouse parvovirus, murine rotavirus, pneumonia

Received: 5/13/04. Revision requested: 6/09/04. Accepted: 6/22/04.
Section of Comparative Medicine, Yale University School of Medicine, New Haven Connecticut 06520-8016.
**Corresponding author.*

virus of mice, reovirus, Sendai virus, and *Mycoplasma pulmonis*, and were free of opportunistic and pathogenic bacteria and parasites on arrival. All animal procedures were approved by the Yale Animal Care and Use Committee, and animal care was in accordance with the NIH *Guide for the Care and Use of Laboratory Animals*. Mice were housed in a quarantine facility, and room conditions included negative pressure differential relative to the corridor, a 12:12-h light:dark cycle, and 10 to 15 air changes/h. Mice were housed on sterilized corncob bedding in sterilized cages (Polysulfone Standard Mouse Cage, ACE, Allentown, Pa.) equipped with stainless steel wire bar tops and filtered cage tops. Mice were fed sterilized standard rodent chow (Purina Mills, 5010, PMI, St. Louis, Mo.) and hyperchlorinated water ad libitum, using a water bottle.

Experimentally induced infection. A *Helicobacter*-free MHV-Y stock was produced and confirmed to be *Helicobacter*-free based on results of PCR analysis, as described (10). Mice were inoculated orally with 20 µl of MHV-Y (300 median mouse infectious doses) and were observed daily for clinical signs of infection.

Sample collection. Fecal samples were collected from mice prior to virus inoculation, on postinoculation day (PID) 15, and on PID 29 for MHV reverse transcriptase (RT)-PCR and *Helicobacter* PCR analyses. *Helicobacter* DNA was not detected at any time point. Additionally, at the times indicated (see Results), feces were collected from mice, which were then euthanized by CO_2 inhalation. After euthanasia, whole blood was collected and necropsy was performed. Feces and whole blood were tested for MHV RNA by RT-PCR analysis, and sera were obtained and stored. Small intestine, cecum, colon, Peyer's patches, mesenteric lymph nodes (MLN), liver, brain, nasal epithelia, cervical lymph nodes, salivary glands, spleen, kidneys, pancreas, lungs, heart, and uterus were examined for gross lesions, and a portion of each tissue was fixed in neutral-buffered 10% formalin and embedded in paraffin.

Histologic examination and in situ hybridization. Five-micron-thick paraffin sections of the aforementioned tissues were stained with hematoxylin and eosin (H&E) for histologic examination or were subjected to in situ hybridization (ISH) to detect MHV RNA. The ISH procedure, using a random-primed ^{32}P-labeled DNA probe transcribed from a gel-purified MHV-JHM N gene fragment, was performed as described (1). Biotin-labeled probes were prepared using the same MHV fragment as template, and selected tissues were hybridized with tyramide signal amplification (12). The ISH signal was scored on a semiquantitative scale under 100-fold magnification as follows: in 0.2 cm of cecal or colonic mucosa, confluent signal = 4, > 20 foci = 3, 11 to 20 foci = 2, and 1 to 10 foci = 1; in 0.2 cm of small intestine, 3 to 5 foci = 2, and 1 to 2 foci = 1; and in MLN or Peyer's patches, > 2 foci = 2 and 1 to 2 foci = 1. Because the frequency of signal varied, the results are reported as the average score for each tissue among all mice examined at a given time point.

Serologic testing. Sera were tested for MHV antibodies by immunofluorescence assay, as described (38), and for IgG, IgM, IgA, IgG_{2a} and IgG_1 by use of an ELISA at dilutions of 1:50 or 1:100 in 0.5% bovine serum albumin (BSA) in phosphate-buffered saline (PBS). Immunoplate wells (Nalge Nunc, Rochester, N.Y.) were coated overnight with 150 ng of purified, bacterially expressed MHV-1 N protein diluted in PBS. Wells were blocked with 1% BSA in PBS for 1 h prior to addition of sera. Plates containing diluted sera were incubated for 1 to 2 h, washed, then incubated for 1 h with horseradish peroxidase-conjugated goat anti-mouse immunoglobulin diluted 1:6,000, anti-IgA, IgG_1, and IgG_{2a} at a dilution of 1:2,000, and anti-IgM diluted 1:4,000 (Serotec, Raleigh, N.C.). Plates were developed using a 3,3',5,5'-tetramethylbenzidine substrate, and were scanned with an MRX Microplate Reader (Thermo Labsystems, Chantilly, Va.).

PCR and RT-PCR analyses. RNA was extracted from whole blood or feces using the RNeasy kit (Qiagen, Chatsworth, Calif.). MHV RT-PCR was performed using the Superscript One-Step RT-PCR System (Invitrogen, Carlsbad, Calif.), as described with MHV N gene primers (10). RT-PCR products were electrophoresed on 1% agarose gels, stained with ethidium bromide, and visualized by UV illumination.

DNA was extracted from feces using the DNeasy Tissue kit (Qiagen), and PCR analysis was performed using *Taq* polymerase (Roche Molecular Biochemicals, Indianapolis, Ind.) and primers for the *Helicobacter* 16S rRNA gene as described (10). PCR products were electrophoresed on 1% agarose gels, stained with ethidium bromide, and visualized by UV illumination.

Results

Pathogenesis of MHV-Y in adult BALB/c mice. Forty BALB/c mice were inoculated orally with MHV-Y, and five infected mice were necropsied on PID 2, 3, 5, 8, 11, 15, 22, and 29. Two uninoculated control mice were necropsied on PID 2, 5, 8, 15, and 29. Inoculated and uninoculated mice remained clinically normal and free of lesions. Infected mice seroconverted to MHV by PID 8 (Table 1), and isotyping indicated that the anti-MHV immunoglobulin response was predominantly IgG2a. MHV RNA was detected in feces, but not blood of all inoculated mice at all time points. Control mice were seronegative for antibodies to MHV, and blood and feces were negative for MHV RNA (data not shown). Results of ISH indicated that the mice developed acute infection limited to the gastrointestinal tract and associated lymphoid tissue, including the MLN (Table 1), and that viral replication ceased between PID 15 and 22. In a few mice, MHV RNA was detected at the squamoglandular junction of gastric mucosal epithelium on PID 2 and 3 by use of ISH. MHV replication was heaviest at PID 2, particularly in mucosa at the ileocecal junction, and signal decreased substantially by PID 5. Peyer's patches in the ileum and jejunum contained virus-positive cells on PID 2 and 3, usually in perifollicular areas or in overlying epithelial cells (M cells). Small foci of infected cells were seen sporadically in the small intestine through PID 11 and in Peyer's patches of one mouse on PID 15. Infection of cecal and colonic mucosal epithelium persisted through day 15 (Fig. 1, Table 1). Signal was particularly heavy in epithelium overlying lymphoid aggregates in the proximal portion of the colon. Viral RNA was not detected in the gastrointestinal tract at PID 22 or 29 by ISH, although MHV RNA was detected in feces by RT-PCR analysis at both time points. MHV RNA was not detected by ISH in other tissues. Despite extensive viral replication in the mucosal epithelium, little to no inflammation was evident in response to infection.

Pathogenesis of MHV-Y in adult C57BL/6 mice. Twenty-two adult C57BL/6 mice were inoculated orally with MHV-Y. Four mice were necropsied on PID 3, 5, 8, 15, and 22, and two mice were necropsied on PID 29. All inoculated mice had seroconverted by PID 8 (Table 2), and isotyping indicated that the anti-MHV immunoglobulin response was IgG2a specific.

Table 1. Pathogenesis of mouse hepatitis virus strain Y (MHV-Y) in adult BALB/c mice

	In situ hybridization[a]						MHV-RT-PCR[b]		Serology[c]
PID	SI	Stom	Ceca	Colon	MLN	PP	Feces	Blood	
2	1.80	0.20	2.80	2.25	1.00	1.00	5/5	0/5	0/5
3	1.10	0.20	1.60	2.20	1.60	1.00	5/5	0/5	0/5
5	0.25	0.00	1.00	1.80	0.35	0.75	5/5	0/5	0/5
8	0.00	0.00	0.00	1.00	0.00	0.00	5/5	0/5	5/5
11	0.10	0.00	0.00	1.20	0.00	0.00	5/5	0/5	5/5
15	0.00	0.00	1.00	1.60	0.00	0.60	5/5	0/5	5/5
22	0.00	0.00	0.00	0.00	0.00	0.00	5/5	0/5	5/5
29	0.00	0.00	0.00	0.00	0.00	0.00	5/5	0/5	5/5

[a]Average of hybridization scores. Scores for ceca/colon were determined per 1/5 cm at 100-fold magnification: confluent signal = 4, > 20 foci = 3, 11 to 20 foci = 2, 1 to 10 foci = 1, and 0 foci = 0. Scores for stomach and small intestine were determined per 1/5 cm at 100-fold magnification: 3 to 5 foci = 2, and 1 to 2 foci = 1. Scores for PP and MLN were determined by the number of positive foci per 100-fold magnification: > 2 foci = 2, 1-2 foci =1.
[b]Number of MHV-RT-PCR-positive samples/number of samples tested.
[c]Number of MHV seropositive samples/number of samples tested.
PID = postinoculation day; RT-PCR = reverse transcriptase-polymerase chain reaction analysis; SI = small intestine; Stom = Stomach; MLN = mesenteric lymph nodes; PP = Peyer's patches.

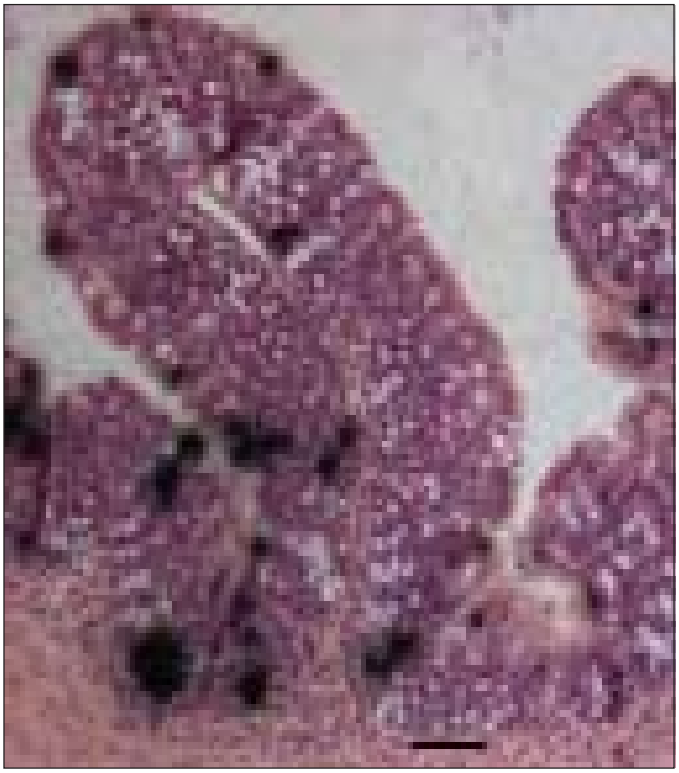

Figure 1. In situ hybridization using radioactively labeled mouse hepatitis virus (MHV) probe of the proximal portion of the colon in a MHV-Y-infected BALB/c mouse on postinoculation day (PID) 3. Signal is associated with surface and crypt epithelium. H&E stain; bar = 50 μm.

MHV RNA was detected in feces, but not blood of all inoculated mice through PID 22. Inoculated and uninoculated mice remained clinically normal and free of gross lesions.

The pathogenesis of MHV-Y infection in C57BL/6 mice closely resembled that in BALB/c mice in that signal intensity and tissue distribution were similar to those seen in BALB/c mice through PID 15 (Table 2). Infected cells were no longer detected in the small intestine or MLN after PID 8 or in the cecum after PID15. However, MHV RNA was still present in colonic mucosal epithelium at PID 22. MHV RNA was detected in feces at PID 22, but not at PID 29. Two uninoculated control mice necropsied on PID 3 were seronegative for antibodies to MHV, and feces and blood were negative for MHV RNA by RT-PCR analysis (data not shown).

Pathogenesis of MHV-Y in B cell-deficient mice. Twenty-two B cell-deficient μMT mice were inoculated orally with MHV-Y to investigate the role of B cells in virus clearance. Four mice were necropsied on PID 3, 5, 8, 15, and 22, and two mice were necropsied on PID 29. As expected, inoculated mice did not develop antibodies against MHV (Table 3). RT-PCR analysis detected MHV-RNA in feces, but not in blood from all inoculated mice necropsied on PID 3–29. Virus was not found in blood or feces of control mice necropsied on PID 3, and all mice remained clinically normal and free of gross lesions.

MHV-Y RNA was restricted to the gastrointestinal tract and MLN of infected mice (Table 3). Virus-positive cells in gastric mucosa were localized to the squamoglandular junction at PID 5 (Fig. 2), and were found in duodenal Brunner's glands of one mouse on PID 8. Small intestine had consistent evidence of low-level infection for the duration of the experiment. It had scattered foci of infected cells, which were more concentrated in epithelium overlaying small, infrequently observed Peyer's patches. The ileocecal junction was more heavily infected than small intestine at all time points examined. Colonic epithelium also was heavily infected; many areas had confluent mucosal signal by PID 3. Additionally, signal was most intense in the proximal portion of the colon at all time points, with two to three times the number of infected cells in this area compared with the remainder of the colon. Although B cell-deficient mice remained clinically normal, they had delayed virus clearance from the gastrointestinal tract.

Because an end point for viral clearance from μMT mice was not reached by PID 29, a second experiment extended ISH examination to PID 50 and RT-PCR analysis through PID 120 (Table 3). Infection on PID 8–29 was similar to that seen previously (data not shown). Mice sustained low-level infection in mucosal epithelium of the small intestine, cecum, and colon through PID 50 (Fig. 3). Gut-associated lymphoid tissue (GALT) was rarely seen and did not contain viral signal. Results of fecal RT-PCR analysis were positive through PID 57.

Pathogenesis of MHV-Y in T cell-deficient mice. Twenty-two T cell-deficient Tcrβδ$^-$ mice were inoculated orally with MHV-Y to investigate the role of T cells in virus clearance. Four mice were necropsied on PID 3, 5, 8, 15, and 22, and two mice were necropsied on PID 29. Uninoculated control mice did not seroconvert to MHV, and MHV RNA was not detected in blood or feces. Of 14 inoculated mice necropsied on PID 8 or later, 10 developed antibodies to MHV (Table 4). However, sera from these mice were weakly reactive against MHV antigens compared

Table 2. Pathogenesis of MHV-Y in adult C57BL/6 mice

	In situ hybridization						MHV-RT-PCR		Serology
PID	SI	Stom	Ceca	Colon	MLN	PP	Feces	Blood	
3	1.75	0.0	2.75	3.00	0.75	0.0	4/4	0/4	0/4
5	1.50	0.0	1.50	2.50	0.75	0.37	4/4	0/4	0/4
8	0.25	0.0	0.25	2.25	0.16	0.0	4/4	0/4	4/4
15	0.0	0.0	0.37	1.00	0.0	0.0	4/4	0/4	4/4
22	0.0	0.0	0.0	0.37	0.0	0.0	4/4	0/4	4/4
29	0.0	0.0	0.0	0.0	0.0	0.0	0/2	0/2	2/2

See Table 1 for explanation of abbreviations and data presentation.

Table 3. Pathogenesis of MHV-Y in adult μMT mice

	In situ hybridization						MHV-RT-PCR		Serology
PID	SI	Stom	Ceca	Colon	MLN	PP	Feces	Blood	
3[a]	1.00	0.0	2.62	4.00	0.75	ND	4/4	0/4	0/4
5[a]	0.75	0.25	1.25	2.37	1.25	ND	4/4	0/4	0/4
8[a]	0.50	0.25	1.75	2.62	0.0	0.0	4/4	0/4	0/4
15[a]	0.50	0.0	1.00	1.00	0.25	ND	4/4	0/4	0/4
22[a]	0.75	0.0	0.82	1.50	0.0	0.0	4/4	0/4	0/4
29[a]	0.50	0.0	0.50	1.00	ND	0.0	2/2	0/2	0/2
36[b]	0.625	0.0	0.875	0.25	0.0	0.0	4/4	0/4	0/4
43[b]	0.75	0.0	0.75	0.625	0.0	0.0	4/4	0/4	0/4
50[b]	0.6	0.0	0.75	0.8	0.0	0.0	5/5	0/5	0/5

[a]Data from experiment 1.
[b]Data from experiment 2.
ND = Not determined.
See Table 1 for explanation of abbreviations and data presentation.

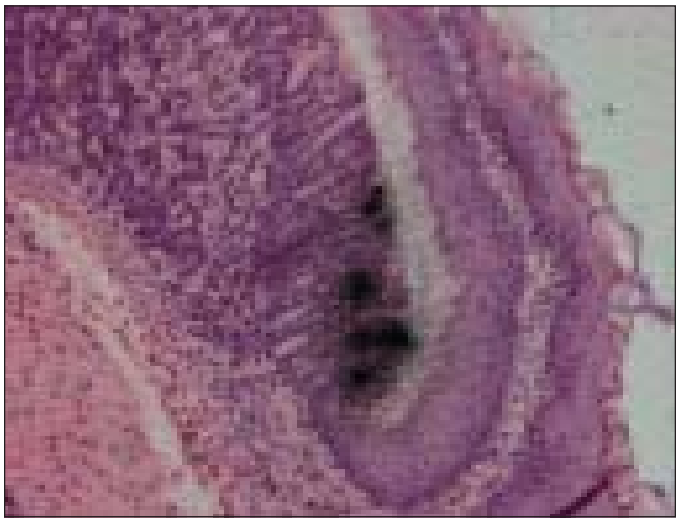

Figure 2. In situ hybridization using radioactively labeled MHV probe of the stomach in an MHV-Y-infected, B cell-deficient μMT mouse on PID 5. Signal is prominent in mucosal epithelium at the squamoglandular junction. H&E stain; magnification, ×75.

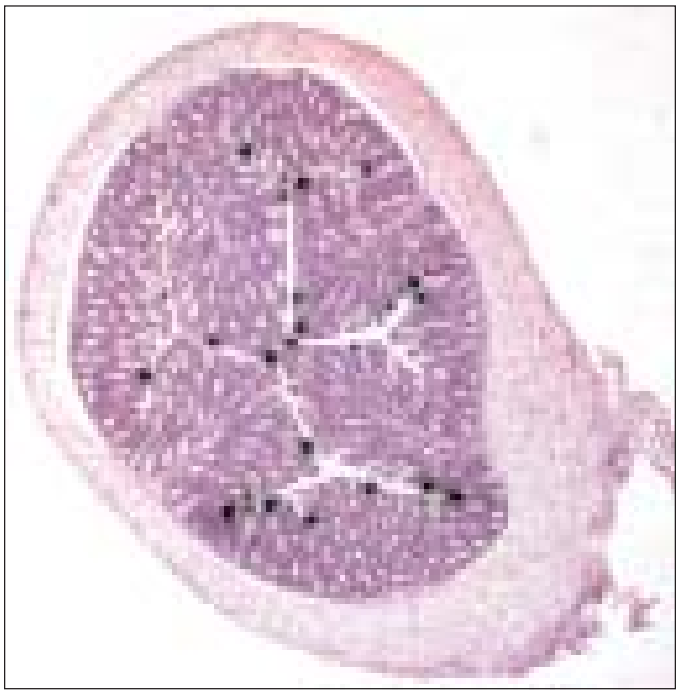

Figure 3. In situ hybridization using radioactively labeled MHV probe of the colon in an MHV-Y-infected, B cell-deficient μMT mouse on PID 50. Signal is shown in surface epithelium. H&E stain; magnification, ×15.

with sera from immunocompetent mice. Isotyping detected low concentration of anti-MHV IgM between PID 8 and 29 in 5 of 12 of the T cell-deficient mice (data not shown). MHV RNA was detected in feces of all inoculated mice throughout the experiment and in blood from half of the mice necropsied on PID 8 and all mice necropsied at later time points, indicating development of chronic viremia.

Inoculated mice began to manifest signs of clinical illness, including hunching and dehydration, on PID 22, and had severe disease by PID 29. Results of ISH indicated that, although infection was confined to the gastrointestinal tract through PID 8, it became disseminated by PID 15. On PID 8, heaviest signal was associated with perifollicular areas of colonic lymphoid aggregates (Table 4), predominantly among large cells that were morphologically consistent with macrophages. Signal in MLN also was localized to perifollicular regions. On day 15, viral dissemination was associated with peritonitis, accompanied by prominent ISH signal, especially in the capsule and subjacent parenchymal of visceral organs and in the mesentery (Fig. 4). Signal also was present in the mediastinal lymph nodes of two mice and in the spleen of a third mouse, suggesting that virus

Table 4. Pathogenesis of MHV-Y in adult Tcrβδ- mice

	In situ hybridization						MHV-RT-PCR		Serology
PID	SI	Stom	Ceca	Colon	MLN	PP	Feces	Blood	
3	1.25	0.00	2.50	3.25	1.00	0.16	4/4	0/4	0/4
5	1.25	0.25	1.25	1.87	1.50	0.25	4/4	0/4	0/4
8	1.00	0.50	1.25	1.60	1.50	1.30	4/4	2/4	2/4
15	1.66	1.00	1.25	2.25	1.50	0.66	4/4	4/4	4/4
22	1.33	0.62	1.50	2.75	2.00	0.66	4/4	4/4	3/4
29	2.00	0.50	1.50	3.50	2.00	1.00	2/2	2/2	1/2

See Table1 for explanation of abbreviations and data presentation.

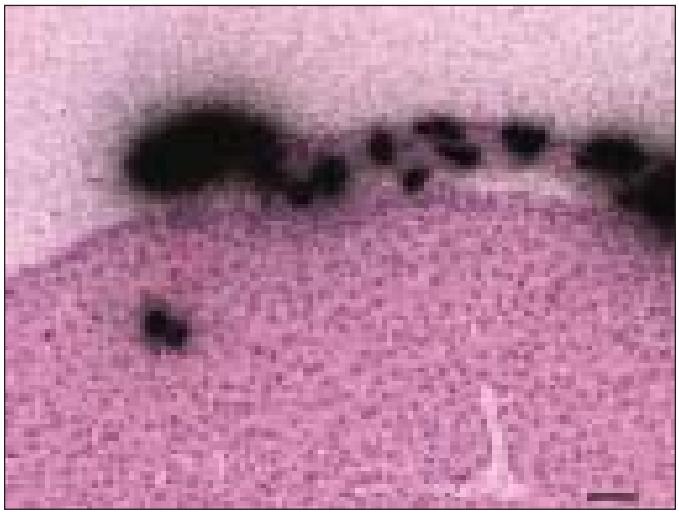

Figure 4. In situ hybridization using radioactively labeled MHV probe of the liver in an MHV Y-infected, T cell-deficient Tcrβδ- mouse on PID 22. Signal is shown on the capsule of the liver and in associated mesentery. H&E stain; bar = 50 μm.

may have spread via the lymphatic network. Although virus was most evident in the gastrointestinal tract and associated lymphoid tissue through PID 22, it was detected in all organs examined, including brain, liver, spleen, kidneys, lungs, bladder, pancreas, uterus, heart, and salivary glands, by PID 29 (Fig. 5).

To attempt to identify specific cell types infected by MHV, selected tissues from a T cell-deficient mouse at PID 29 were hybridized with a biotinylated probe. Results confirmed infection in gastrointestinal tract epithelium, with signal evident in individual epithelial cells and in multinucleated syncytia (Fig. 6A). Necrotic infected cells and syncytia were shed into the luminal space of the colon, and labeled plaques of residual MHV RNA were located along the apical surfaces of the mucosa (Fig. 6B). Positive cells were also located within lymphoid aggregates in colon and Peyer's patches of the small intestine. Foci of infection appeared to consist of aggregates of infected cells or syncytia (Fig. 6C). The MHV RNA-positive cells in the mesentery often colocalized with lymphocytic infiltrates. (Fig. 6D).

Discussion

Previous pathogenesis studies of enterotropic MHV strains analyzed infection by histologic examination and infant mouse bioassay for infectious virus. Given the minimal cytopathic effects caused by these agents and the inability of infant mouse bioassay to localize virus, these methods were unable to determine the specific cell tropisms in the gastrointestinal tract. Sensitive molecular hybridization techniques were used in the experiments of this study to determine the distribution and course of enterotropic infection. Using these technologies, high levels of viral RNA were detected at PID 2 and 3, indicating early infection of all tissues in the gastrointestinal tract. Also, viral RNA was frequently detected when cytopathic effects were not evident microscopically.

Host genotype affects the outcome of some polytropic MHV infections. The most pronounced example is the resistance of SJL mice to central nervous system infection by polytropic MHV-JHM (19, 41), which has been attributed to absence of an MHV receptor allele, murine carcinoembryonic antigen-related adhesion molecule 1a, in SJL mice (8, 48, 49). Additionally, resistance of A/J mice to liver necrosis caused by polytropic MHV-3 is due to their inability to produce a unique monocyte procoagulant activity in response to MHV-3 infection (23, 24). However, genetic influences on polytropic MHV infection in BALB/c and C57BL/6 mice appear to be minor (19-21, 39, 41, 44).

The role of host genotype on the outcome of enterotropic MHV infection is not well established. In studies comparing MHV-Y infection of BALB/c and SJL mice, the infection was similar in extent and duration (3). Nevertheless, differences in antibody responses during enterotropic MHV infection and duration of virus transmission in C57BL/6 and BALB/c mice have been noted. Intranasal infection with MHV-NuU resulted in higher titer of MHV-specific antisera in C57BL/6 than BALB/c mice (33). After oral MHV-Y inoculation, C57BL/6 mice transmitted virus for 2 weeks, whereas BALB/c mice transmitted virus for 4 weeks (10). In the study reported here, viral RNA was detected in the colon and feces of C57BL/6 mice through 3 weeks, although results of a previous transmission study indicated transmission to contact sentinels for only 2 weeks (10). This suggests that viral RNA detected at later time points was noninfectious or that the concentration of infectious virus excreted after 2 weeks in the previously reported study was below the threshold required to initiate infection. Viral RNA was detected in the gastrointestinal tract of BALB/c mice by ISH and RT-PCR analysis through PID 15, yet fecal samples were MHV RNA positive through PID 29. This finding supports documentation that MHV-Y-inoculated BALB/c mice can transmit infection through soiled bedding for 4 weeks (10). Thus, BALB/c mice may shed infectious virus for longer periods than do C57BL/6 mice, even though infection of cecal or colonic mucosa was not detected beyond 3 weeks by ISH. Small sample size and non-uniform distribution of infected cells may have contributed to negative ISH results at the later time points. Although BALB/c and C57BL/6 mice had similar patterns of seroconversion to MHV, we cannot rule out the possibility that differences in neutralizing antibody secretion in the intestine contributes to differences in virus detection and transmission (i.e., neutralizing antibody responses in C57BL/6 mice were stronger than those in BALB/c mice).

In B cell-deficient μMT mice, strain MHV-Y caused chronic in-

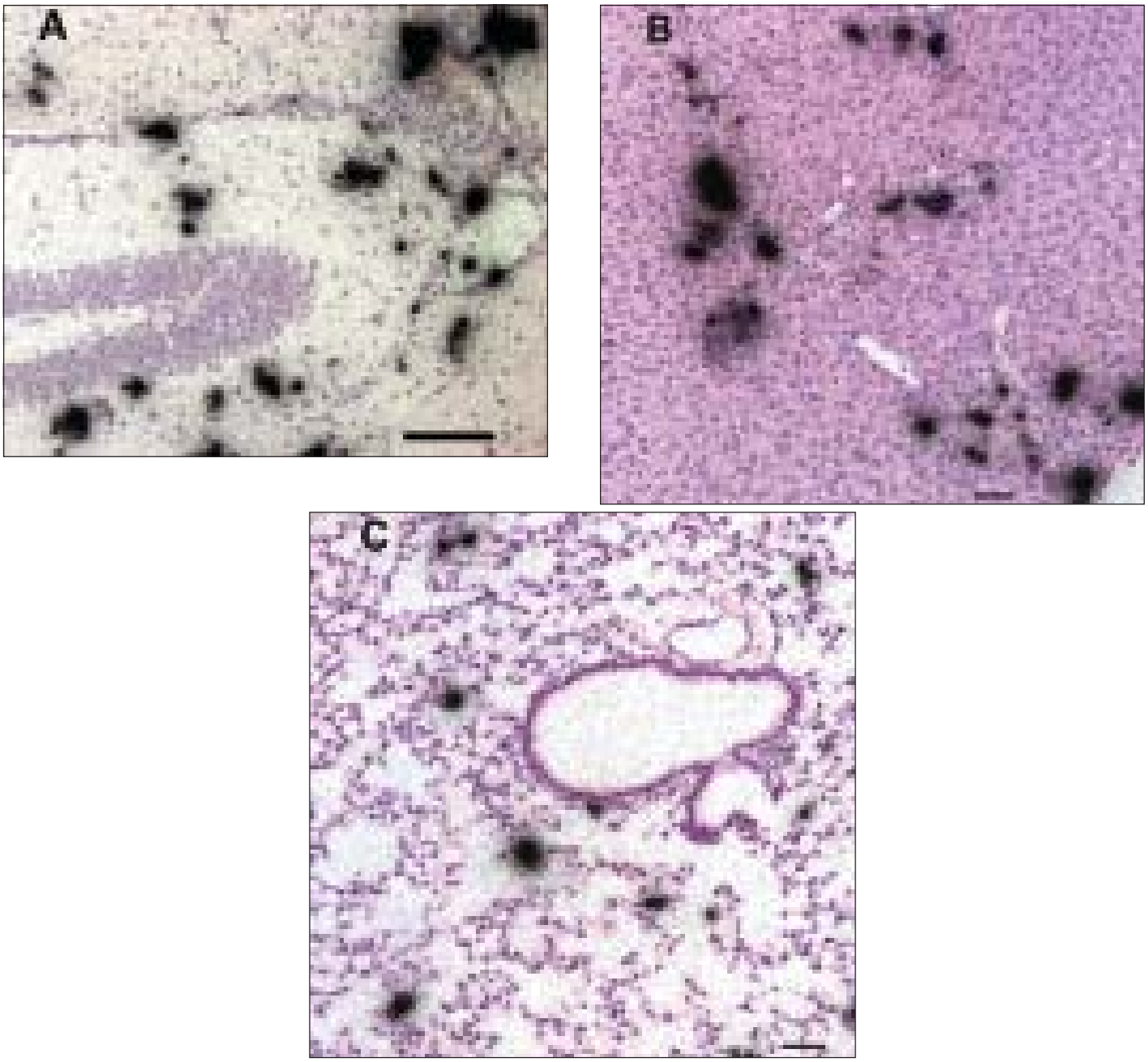

Figure 5. In situ hybridization using radioactively labeled MHV probe in an MHV-Y-infected T cell-deficient Tcrβδ$^-$ mouse on PID 29. (A) Brain, (B) liver, and (C) lung. H&E stain; bar = 50 μm.

fection that was localized to the gastrointestinal tract. We attribute delayed clearance of MHV from the intestine principally to the absence of an anti-MHV humoral response, although other immune defects may have contributed to this effect. For example, μMT mice have decreased Th2 cytokines (interleukin 4, interleukin 10, and interferon-γ) and T-cell growth factor β in GALT (16). Previous studies indicate that interferon-γ plays an important role in MHV clearance (11). Also, these mice lack B cell-mediated cytolysis, an antibody-independent, natural killer cell-like process, in which B cells lyse MHV-infected cells following interaction of the MHV receptor on B cells with MHV S protein expressed on infected cells (32, 47). In addition, μMT mice are unable to produce mucosal antibodies, have decreased size and number of Peyer's patches with abnormal follicle-associated epithelium overlying the Peyer's patches, and decreased follicular dendritic cell networks within Peyer's patches (15). Despite these deficiencies, remaining immune components (T cells, macrophages, natural killer cells) were sufficient to prevent viral dissemination and disease, and eventually resulted in MHV-Y clearance.

The inability of μMT mice to control infections has been reported for several viral systems (6, 9, 31, 43), including neurotropic MHV-JHM and hepatotropic MHV-A59 (26, 30). Compared with that in control mice, infection with MHV-JHM in μMT mice results in chronic, fatal encephalitis accompanied by reduced T-cell responses in brain (5, 26). Intracerebral or intrahepatic inocu-

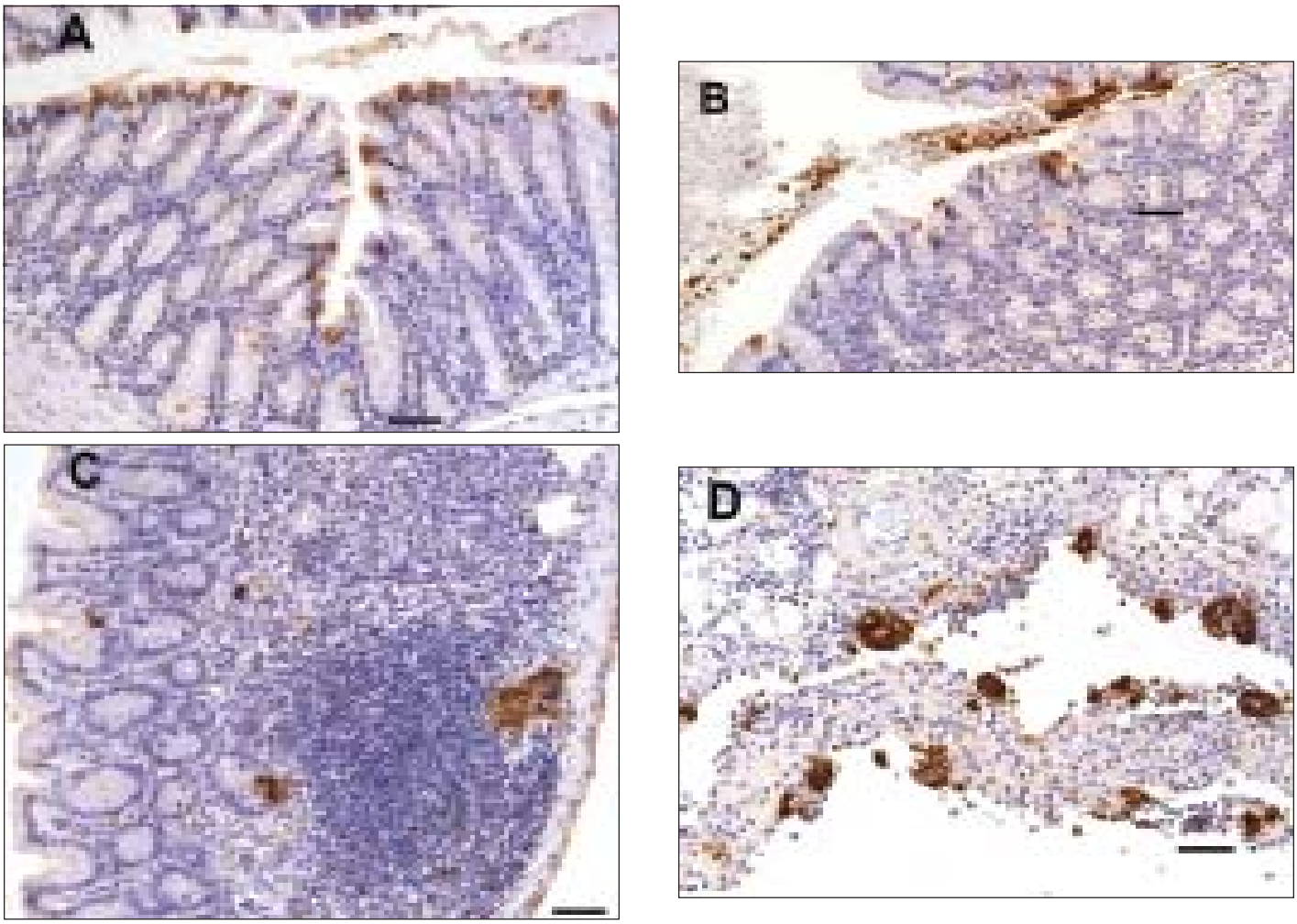

Figure 6. In situ hybridization using biotinylated MHV probe (brown substrate) of an MHV-Y- infected, T cell-deficient Tcrβδ$^-$ mouse on PID 29. (A) Infected colonic epithelium. (B) Colonic syncytia and sloughed MHV-infected cells in the lumen of the colon. (C) Colonic lymphoid tissue with labeled cells in the perifollicular region. (D) Severe peritonitis accompanied by virus infection. H&E stain; bar = 50 μm.

lation of MHV-A59 in μMT mice results in acute infection of the liver and chronic infection of the central nervous system, with high amounts of virus replication in the spinal cord and brain through PID 148 (30). A similar pattern of liver and central nervous system infection also was seen in antibody-deficient JhD and mIgM transgenic mice, indicating that antibodies, in contrast to other B-cell functions, are essential for viral clearance from the central nervous system (30). The rapid clearance of MHV from the liver was not restricted to a single genetic background and was attributed to the regenerative capacity of the liver (30). Although the intestine also has high regenerative capacity, we did not observe rapid clearance of MHV-Y from the intestine of μMT mice. In fact, the high regenerative capacity of the intestine may have provided a renewable substrate for MHV replication.

In T cell-deficient Tcrβδ$^-$ mice, MHV-Y caused chronic, disseminated, fatal infection. In contrast to immunocompetent and μMT mice, where viral RNA levels in tissues peaked at PID 8, viral levels in the gastrointestinal tract of Tcrβδ$^-$ mice continued to increase through PID 29. This increase in viral RNA also occurred in MLN, where immune cells appeared to be ineffective at eliminating infection and may have served as a means of virus dissemination to multiple organs. Virus-infected cells in lymphoid tissues and mesenteric infiltrates preceded widespread dissemination, suggesting that lymphocytes may be important for viral spread. The Tcrβδ$^-$ mice were viremic on PID 8 and later times, and it is unclear whether virus was present in the fluid and cellular compartments of blood, including B lymphocytes and monocytes. Previous reports suggest that infection of B lymphocytes may be virus strain dependent. Strains MHV-3 and MHV-N have been reported to readily infect B lymphocytes (22), whereas B lymphocytes appear to be resistant to MHV-JHM infection (27, 34, 40). In contrast, infection of macrophages with polytropic and enterotropic MHV strains has been widely documented (2, 20, 22, 39, 45). The distribution of viral signal in GALT was consistent with infection of macrophages and lymphocytes, and the peritonitis/serositis observed at PID 15 was similar to that previously seen in interferon-γ-deficient mice (11). Thus, as suggested previously for mucosal epithelium, recruitment of virus-susceptible (lymphoid) cells to the gastrointestinal tract and mesentery may have provided an additional substrate for viral replication. Recruitment of immune cell populations to the intestine and associated lymphoid tissues has been documented for other intestinal infections in Tcrβδ$^-$ mice. For example, murine rotavirus infection of Tcrβδ$^-$ mice induces

hyperproliferation and activation of B lymphocytes in the MLN and Peyer's patches (7).

Our experiments in Tcrβδ$^-$ mice confirm that T-cell deficiency results in an inability to control the dissemination of MHV. Infected mice were unable to generate a strong humoral immune response against MHV because they lacked Th1 lymphocyte-mediated B-cell help and had impaired antibody class switching. Altered humoral immune responses to other viruses in Tcrβδ$^-$ mice have been documented. For example, they do not produce a neutralizing IgG response against vesicular stomatitis virus (28). In contrast, polyomavirus infection induces a protective T cell-independent IgM and IgG response in Tcrβδ$^-$ mice (42), and murine rotavirus infection of Tcrβδ$^-$ mice, which is rapidly resolved and induces production of low concentration of anti-rotaviral fecal IgA and excretion of low concentration of anti-rotaviral IgM in cultured Peyer's patches (13). Further, chronic wasting disease has been repeatedly reported (11, 14, 25, 29, 36, 46, 50) during infections of athymic nude mice with enterotropic MHV strains. Finally, mice deficient in interferon-γ, a Th1 cell-induced cytokine, develop severe disseminated disease with extensive peritonitis and adhesions (11). Although this study in Tcrβδ$^-$ mice indicated viral dissemination and formation of peritonitis, these mice succumbed quickly to the infection without development of diarrhea, ascites, or adhesions.

In conclusion, these experiments support the concept that B cells promote clearance of enterotropic MHV strains from intestinal mucosa and that T cells are required to prevent dissemination of enterotropic MHV strains from the gastrointestinal tract and GALT. Outbreaks of MHV in contemporary mouse colonies, which include many immunodeficient, genetically engineered mice, can lead to multiple clinical outcomes. Our results suggest that mice with deficiencies in T cell-mediated immunity will likely develop lethal MHV infection in response to strains of enterotropic MHV that may be non-pathogenic for immunocompetent adult mice. Furthermore, mice with deficiencies in humoral immunity may chronically transmit virus. Additional studies will be needed to more accurately determine the role of infection of immune cell populations in the pathogenesis of enterotropic MHV infections.

Acknowledgments

This research was funded by a grant from the American College of Laboratory Animal Medicine. We thank Carmen Booth for assistance with photography.

References

1. **Ball-Goodrich, L. J., S. E. Leland, E. A. Johnson, F. X. Paturzo, and R. O. Jacoby.** 1998. Rat parvovirus type 1: the prototype for a new rodent parvovirus serogroup. J. Virol. **72:**3289-3299.
2. **Bang, F. B. and A. Warwick.** 1960. Mouse macrophages as host cells for mouse hepatitis virus and the genetic basis of their susceptibility. Proc. Natl. Acad. Sci. USA **46:**1065-1075.
3. **Barthold, S. W., D. S. Beck, and A. L. Smith.** 1993. Enterotropic coronavirus (mouse hepatitis virus) in mice: influence of host age and strain on infection and disease. Lab. Anim. Sci. **43:**276-284.
4. **Barthold, S. W., A. L. Smith, and M. L. Povar.** 1985. Enterotropic mouse hepatitis virus infection in nude mice. Lab. Anim. Sci. **35:**613-618.
5. **Bergmann, C. C., C. Ramakrishna, M. Kornacki, and S. A. Stohlman.** 2001. Impaired T cell immunity in B cell-deficient mice following viral central nervous system infection. J. Immunol. **167:**1575-1583.
6. **Binder, G. K. and D. E. Griffin.** 2001. Interferon-γ mediated site specific clearance of alphavirus from CNS neurons. Science **293:**303-306.
7. **Blutt, S. E., K. L. Warfield, D. E. Lewis, and M. E. Connor.** 2002. Early response to rotavirus infection involves massive B cell activation. J. Immunol. **168:**5716-5721.
8. **Boyle, J. F., D. G. Weismiller, and K. V. Holmes.** 1987. Genetic resistance to mouse hepatitis virus correlates with absence of virus-binding activity on target tissues. J. Virol. **61:**185-189.
9. **Brundler, M. A., P. Aichele, M. Bachmann, D. Kitamura, K. Rajewsky, and R. M. Zinkernagel.** 1996. Immunity to viruses in B cell-deficient mice: influence of antibodies on virus persistence and on T cell memory. Eur. J. Immunol. **26:**2257-2262.
10. **Compton, S. R., L. J. Ball-Goodrich, F. X. Paturzo, and J. D. Macy.** 2004. Transmission of enterotropic mouse hepatitis virus from immunocompetent and immunodeficient mice. Comp. Med. **54:**29-35.
11. **Compton, S. R., L. J. Ball-Goodrich, C. J. Zeiss, L. K. Johnson, E. A. Johnson, and J. D. Macy.** 2003. Pathogenesis of mouse hepatitis virus infection in gamma interferon-deficient mice is modulated by co-infection with *Helicobacter hepaticus*. Comp. Med. **53:**197-206.
12. **Compton, S. R., R. O. Jacoby, F. X. Paturzo, and A. L. Smith.** 2004. Persistent Seoul virus infection in Lewis rats. Arch. Virol. **149:**1325-1339.
13. **Franco, M. and H. Greenberg.** 1997. Immunity to rotavirus in T cell deficient mice. Virology **238:**169-179.
14. **Fujiwara, K.** 1988. Persistent mouse hepatitis virus infection in nude mice. Jpn. J. Exp. Med. **58:**115-121.
15. **Golovkina, T. V., M. Shlomchik, L. G. Hannum, and A. Chervonsky.** 1999. Organogenic role of B lymphocytes in mucosal immunity. Science **286:**1965-1968.
16. **Gonnella, P. A., H. P. Waldner, and H. L. Weiner.** 2001. B cell-deficient (μMT) mice have alterations in the cytokine microenvironment of the gut-associated lymphoid tissue (GALT) and a defect in the low dose mechanism of oral tolerance. J. Immunol. **166:**4456-4464.
17. **Homberger, F. R., L. Zhang, and S. W. Barthold.** 1998. Prevalence of enterotropic and polytropic mouse hepatitis virus in enzootically infected mouse colonies. Lab. Anim. Sci. **48:**50-54.
18. **Jacoby, R. O. and J. R. Lindsey.** 1997. Health care for research animals is essential and affordable. FASEB J. **11:**609-614.
19. **Knobler, R. L., M. V. Haspel, and M. B. Oldstone.** 1981. Mouse hepatitis virus type 4 (JHM strains) induced fatal central nervous system disease. I. Genetic control and murine neuron as the susceptible site of disease. J. Exp. Med. **153:**832-843.
20. **Knobler, R. L., L. A. Tunison, and M. B. Oldstone.** 1984. Host genetic control of mouse hepatitis virus type 4 (JHM strain) replication. I. Restriction of virus amplification and spread in macrophages from resistant mice. J. Gen. Virol. **65:**1543-1548.
21. **Kyuwa, S., S. Kawamura, Y. Tagawa, Y. Iwakura, T. Urano, and Y. Yoshikawa.** 2003. Differences between BALB/c and C57BL/6 mice in mouse hepatitis virus replication in primary hepatocyte culture. Exp. Anim. **52:**81-84.
22. **Lamontagne, L. and P. Jolicoeur.** 1994. Low-virulent mouse hepatitis viruses exhibiting various tropisms in macrophages, T and B cell subpopulations, and thymic stromal cells. Lab. Anim. Sci. **44:**17-24.
23. **LePrevost, C., J. L. Virelizier, and J. M. Dupuy.** 1975. Immunopathology of mouse hepatitis type 3 infection. III. Clinical and virological observations of a persistent viral infection. J. Immunol. **115:**640-643.
24. **Levy, G. A., J. L. Leibowitz, and T. S. Edginton.** 1981. Induction of monocyte procoagulant activity in murine hepatitis virus type 3 parallels disease susceptibility in mice. J. Exp. Med. **154:**1150-1163.
25. **Liang, S. C., W. C. Lian, F. J. Leu, P. J. Lee, A. J. Chao, C. C. Hong, and W. F. Chen.** 1995. Epizootic of low-virulence hepatotropic murine hepatitis virus in a nude mice breeding colony in Taiwan. Lab. Anim. Sci. **45:**519-522.

26. **Lin, M. T., D. R. Hinton, N. W. Marten, C. C. Bergmann, and S. A. Stohlman.** 1999. Antibody prevents virus reactivation within the central nervous system. J. Immunol. **162:**7358-7368.
27. **Lin, M. T., S. A. Stohlman, and D. R. Hinton.** 1997. Mouse hepatitis virus is cleared from the central nervous systems of mice lacking perforin-mediated cytolysis. J. Virol. **71:**383-391.
28. **Maloy, K. J., B. Odermatt, H. Hengartner, and R. M. Zinkernagel.** 1998. Interferon gamma-producing gammadelta T cell-dependent antibody isotype switching in the absence of germinal center formation during virus infection. Proc. Natl. Acad. Sci. USA **95:**1160-1165.
29. **Matthaei, K. I., J. R. Berry, M. P. France, C. Yeo, J. Garcia-Aragon, and P. J. Russell.** 1998. Use of polymerase chain reaction to diagnose a natural outbreak of mouse hepatitis virus infection in nude mice. Lab. Anim. Sci. **48:**137-144.
30. **Matthews, A. E., S. R. Weiss, M. J. Shlomchik, L. G. Hannum, J. L. Gombold, and Y. Paterson.** 2001. Antibody is required for clearance of infectious murine hepatitis virus A59 from the central nervous system, but not the liver. J. Immunol. **167:**5254-5263.
31. **McNeal, M. M., K. S. Barone, M. N. Rae, and R. L. Ward.** 1995. Effector functions of antibody and $CD8^+$ cells in resolution of rotavirus infection and protection against reinfection in mice. Virology **214:**387-397.
32. **Morales, S., B. Parra, C. Ramakrishna, D. M. Blau, and S. A. Stohlman.** 2001. B-cell-mediated lysis of cells infected with the neurotropic JHM strain of mouse hepatitis virus. Virology **286:**160-167.
33. **Nakanaga, K., T. Ishida, and K. Fujiwara.** 1983. Differences in antibody production against mouse hepatitis virus (MHV) among mouse strains. Lab. Anim. **17:**90-94.
34. **Parra, B., D. R. Hinton, N. W. Marten, C. C. Bergmann, M. T. Lin, C. S. Yang, and S. A. Stohlman.** 1999. IFN-gamma is required for viral clearance from central nervous system oligodendroglia. J. Immunol. **162:**1641-1647.
35. **Rehg, J., M. Blackman, and L. Toth.** 2001. Persistent transmission of mouse hepatitis virus by transgenic mice. Comp. Med. **51:**369-374.
36. **Sebesteny, A. and A. C. Hill.** 1974. Hepatitis and brain lesions due to mouse hepatitis virus accompanied by wasting in nude mice. Lab. Anim. **8:**317-326.
37. **Shames, B., J. G. Fox, F. Dewhirst, L. Yan, Z. Shen, and N. S. Taylor.** 1995. Identification of widespread *Helicobacter hepaticus* infection in feces in commercial mouse colonies by culture and PCR assay. J. Clin. Microbiol. **33:**2968-2972.
38. **Smith, A. L.** 1983. An immunofluorescence test for detection of serum antibody to rodent coronaviruses. Lab. Anim. Sci. **33:**157-160.
39. **Smith, M. S., R. E. Click, and P. G. Plagemann.** 1984. Control of mouse hepatitis virus replication in macrophages by a recessive gene on chromosome 7. J. Immunol. **133:**428-432.
40. **Stohlman, S. A., C. C. Bergmann, M. T. Lin, D. J. Cua, and D. R. Hinton.** 1998. CTL effector function within the central nervous system requires $CD4^+$ T cells. J. Immunol. **160:**2896-2904.
41. **Stohlman, S. A. and J. A. Frelinger.** 1978. Resistance to fatal central nervous system disease by mouse hepatitis virus, strain JHM. I. Genetic analysis. Immunogenetics **6:**277-281.
42. **Szomolanyi-Tsuda, E., J. D. Brien, J. E. Dorgan, R. L. Garcea, R. T. Woodland, and R. M. Welsh.** 2001. Antiviral T-cell-independent type 2 antibody responses induced in vivo in the absence of T and NK cells. Virology **280:**160-168.
43. **Thomsen, A. R., J. Johansen, O. Marker, and J. P. Christensen.** 1996. Exhaustion of CTL memory and recrudescence of viremia in lymphocytic choriomeningitis virus-infected MHC class II-deficient mice and B cell-deficient mice. J. Immunol. **157:**3074-3080.
44. **van der Veen, R. C.** 1996. Immunogenicity of JHM virus proteins: characterization of $CD4^+$ T cell epitope on nucleocapsid protein induces different T-helper subsets. Virology **225:**339-346.
45. **Virelizier, J. L. and A. C. Allison.** 1976. Correlation of persistent mouse hepatitis virus (MHV-3) infection with its effect on mouse macrophage cultures. Arch. Virol. **50:**279-285.
46. **Ward, J. M., M. J. Collins, Jr., and J. C. Parker.** 1977. Naturally occurring mouse hepatitis virus infection in the nude mouse. Lab. Anim. Sci. **27:**372-376.
47. **Welsh, R. M., M. V. Haspel, D. C. Parker, and K. V. Holmes.** 1986. Natural cytotoxicity against mouse hepatitis virus-infected cells. II. A cytotoxic effector cell with a B lymphocyte phenotype. J. Immunol. **136:**1454-1460.
48. **Williams, R. K., G. S. Jiang, and K. V. Holmes.** 1991. Receptor for mouse hepatitis virus is a member of the carcinoembryonic antigen family of glycoproteins. Proc. Natl. Acad. Sci. U. S. A. **88:**5533-5536.
49. **Williams, R. K., G. S. Jiang, S. W. Snyder, M. F. Frana, and K. V. Holmes.** 1990. Purification of the 110-kilodalton glycoprotein receptor for mouse hepatitis virus (MHV)-A59 from mouse liver and identification of a nonfunctional, homologous protein in MHV-resistant SJL/J mice. J. Virol. **64:**3817-3823.
50. **Yanagisawa, T., K. Nakanaga, S. Kyuwa, and K. Fujiwara.** 1985. Ascitic disease in nude mice infected with mouse hepatitis virus. Jpn. J. Vet. Sci. **47:**171-174.